

## SOLID-STATE CO-EXTRUSION OF NYLON 6 GEL(U)

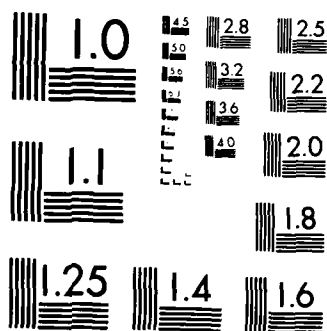
MASSACHUSETTS UNIV AMHERST DEPT OF POLYMER SCIENCE AND

ENGINEERING H H CHUAH ET AL. 25 MAR 85 TR-24

F/G 13/8

NL

[illegible]



MICROCOPY RESOLUTION TEST CHART  
NATIONAL BUREAU OF STANDARDS 1963 A

7  
H

AD-A156 187

OFFICE OF NAVAL RESEARCH

Contract N00014-77-C-1234

Task No. NR 056-123

TECHNICAL REPORT NO. 24

Solid-State Co-Extrusion of Nylon 6 Gel

by

Hoe Hin Chuah and Roger S. Porter

Submitted for Publication

in the British journal, POLYMER

Materials Research Laboratory  
Polymer Science and Engineering Department  
University of Massachusetts  
Amherst, Massachusetts 01003

DTIC  
SELECTE  
JUL 05 1985  
S D  
G

March 25, 1985

Reproduction in whole or in part is permitted for  
any purpose of the United States Government

This document has been approved for public release  
and sale; its distribution is Unlimited

DTIC FILE COPY

REPORT DOCUMENTATION PAGE		READ INSTRUCTIONS BEFORE COMPLETING FORM
1. REPORT NUMBER Technical Report No. 24	2. GOVT ACCESSION NO. AN-4156 1M	3. RECIPIENT'S CATALOG NUMBER
4. TITLE (and Subtitle) Solid-State Co-Extrusion of Nylon 6 Gel		5. TYPE OF REPORT & PERIOD COVERED Interim
		6. PERFORMING ORG. REPORT NUMBER
7. AUTHOR(s) Hoe Hin Chuah and Roger S. Porter		8. CONTRACT OR GRANT NUMBER(s) N00014-83-K-0228
9. PERFORMING ORGANIZATION NAME AND ADDRESS Polymer Science and Engineering University of Massachusetts Amherst, Massachusetts 01003		10. PROGRAM ELEMENT, PROJECT, TASK AREA & WORK UNIT NUMBERS
11. CONTROLLING OFFICE NAME AND ADDRESS Office of Naval Research 800 North Quincey Street Arlington, Virginia 22217		12. REPORT DATE March 25, 1985
		13. NUMBER OF PAGES
14. MONITORING AGENCY NAME & ADDRESS (if different from Controlling Office)		15. SECURITY CLASS. (of this report) Unclassified
		15a. DECLASSIFICATION DOWNGRADING SCHEDULE
16. DISTRIBUTION STATEMENT (of this Report)  Approved for public release; distribution unlimited		
17. DISTRIBUTION STATEMENT (of the abstract entered in Block 20, if different from Report)		
18. SUPPLEMENTARY NOTES		
19. KEY WORDS (Continue on reverse side if necessary and identify by block number)  Nylon 6; gel; draw ratio; co-extrusion; x-ray diffraction; birefringence; x-ray scattering; orientation		
20. ABSTRACT (Continue on reverse side if necessary and identify by block number) A Nylon 6 gel has been drawn to a ratio 5.7, by a split billet co-extrusion technique. The gel was prepared by dissolving Nylon 6 in benzyl alcohol at 165°C and cooled to gel at room temperature. On removing solvent, preorientation is introduced into the gel with the b-chain axis weakly oriented perpendicular to the gel surface. Drawing produces double orientation as shown by wide-angle x-ray diffraction. One population of the crystals are oriented with chain axes in the draw direction, as in the usual uniaxial drawing. The second population have their chain axes oriented perpendicular to draw direction.		

ABSTRACT

A partially dried Nylon 6 gel has been drawn at 150°C and to draw ratio 5.7X, by a split billet co-extrusion technique in an Instron capillary rheometer. The gel was prepared by dissolving Nylon 6 in benzyl alcohol at 165°C and cooled to gel at room temperature. On removing solvent, preorientation was introduced into the gel with the b-chain axis weakly oriented perpendicular to the gel surface. Drawing produces double orientation as shown by wide-angle x-ray diffraction. One population of the crystals are oriented with chain axes in the draw direction, as in the usual uniaxial drawing. The second population have their chain axes oriented perpendicular to draw direction. From birefringence, wide- and small-angle x-ray scattering studies, a deformation mechanism for the double orientation was proposed. Thermal and mechanical properties were also studied. Annealing at 190°C produced partial reorientation of the second crystals resulting in a more complex orientation.

Accession For	
NTIS GRA&I	<input checked="" type="checkbox"/>
DTIC TAB	<input type="checkbox"/>
Unannounced	<input type="checkbox"/>
Justification	
By	
Distribution/	
Availability Codes	
Dist	Avail and/or Special
A/1	



## INTRODUCTION

Pennings and coworkers<sup>1</sup> reported ultra-high modulus polyethylene fiber of  $>100$  GPa made by a continuous growth technique, in either a Poiseuille or Couette flow. It was recognized that the fiber was produced from a gel layer, where the fibrous seed-crystal was attached. The success of this technique is due to reduced molecular entanglements in the gel and to the efficient stretching of chains in a flow field. Subsequently, the potential of a gel state as a route to high modulus fiber has received considerable attention<sup>2,3</sup>. Smith and Lemstra<sup>4</sup> further extended the technique to ultra-draw a dried, molded or cast polyethylene gel film. Such dried gel was reported to draw well, even up to 20X at room temperature<sup>5</sup>. Other polymers that form gels, polypropylene<sup>6,7</sup> and poly(vinyl alcohol)<sup>8</sup> have also been reported to draw well by this method, resulting in high modulus fibers.

Lloyd<sup>9</sup> noted nearly 60 years ago that gel is one which is easier to recognize than to define. This, to some extent, is still true today. In the present context, gel refers to a macroscopically coherent structure with crystallites acting as spatial junction points, trapping a large amount of solvent.

In general, gels are not formed from a good solvent. Gelation occurs when solubility changes by either varying temperature or adding a poor solvent to a polymer solution<sup>10</sup>. Apart from gelation involving flow mentioned above, polymer can also gel under quiescent conditions as when a hot, semi-dilute solution is rapidly cooled. Gelation of semi-crystalline polymer has long been recognized

as a crystallization process<sup>11</sup>. One molecular chain may form cohesive junction points with others at several loci along the chain to form a molecular network. If the junction is very small, the gel approaches a homogeneous one phase system. With several chain segments arranging in lateral order, the junction can then form micellar crystals. It was suggested by Keller<sup>12</sup> that micellar crystals are responsible for gel formation for polymers such as polyethylene, poly(vinyl chloride) and isotactic polystyrene. Micellar crystals can also be mixed with lamellar crystals, and possibly some with tie molecules giving gel connectedness.

Nylon 6 forms a gel when its solution in hot benzyl alcohol is cooled to room temperature. Stamhuis and Pennings<sup>13</sup> investigated the morphology by electron microscopy and found an interlacement of thin fibrillar crystals of 100 ~ 200 Å lateral dimension, aggregated into ribbons of high aspect ratio. These fibrillar crystals have their chain axis perpendicular to the surface and the hydrogen bond direction in the long axes of the crystal. The interlacement forms entanglements, traps solvent and forms a gel. Gelation in this case is analogous to the gelation of rodlike particles which forms a continuous framework through physical contacts<sup>11</sup>. Thus the fibrillar crystals of Nylon 6 gel does not necessarily have reduced molecular entanglement as in polyethylene gel.

The gel of Nylon 6 was reported to be brittle and could not be drawn<sup>13</sup>. However, the co-extrusion method developed in this laboratory has successfully drawn several brittle polymers<sup>14,21</sup>. By our drawing methods, there is a simultaneous compression and extension in a conical die with the deformed

polymer film supported on each face by a surface of polyoxymethylene coextrudate. We are consequently able to draw a partially dried Nylon 6 gel up to 5.7X. This paper investigates the drawing behavior and properties of the drawn gel. A deformation mechanism is proposed for the observed double orientation.



## EXPERIMENTAL

Pellets of high molecular weight Nylon 6 ( $[\eta] = 4.67$  dl/g in 85% formic acid,  $M_v = 183,000$ , Allied Chemicals) were dissolved in benzyl alcohol at 5 wt % concentration at 165°C. The solution was stirred for 1 hour under a  $N_2$  atmosphere. It was then poured into a petri dish lined with filter paper where it gelled at room temperature. Solvent was subsequently removed by blotting with layers of filter paper applied at ever increasing pressure, up to 40 MPa in a press. This was repeated until a partially dried gel was obtained. Further solvent was removed under vacuum at 40°C to give final gel with ~ 20 wt % solvent.

A 2 mm wide strip of the gel film, dried as above, was placed in the center of a split poly(oxymethylene) billet and co-extruded through a conical die of 20° entrance angle in an Instron capillary rheometer at 150°C<sup>15</sup>. This extrusion temperature was chosen as a convenience as poly(oxymethylene) melts at ~160°C and draws easily up to 8X. Draw ratio was measured from the displacement of lateral markers placed on the gel prior to draw. About 10% solvent remained in the extrudate and was removed in vacuum oven at 100°C for 48 hours.

Thermal behavior was characterized with a Perkin-Elmer Differential Scanning Calorimeter-II (DSC) with heating rate of 10°C/min. Indium and tin were used for calibration. Tensile modulus at 0.1% strain was measured using a floor model Instron tensile tester at a strain rate of 0.01 min<sup>-1</sup>.

Total orientation of the drawn gel was measured by birefringence using an Ehringhaus calcspars compensator. As the drawn gel developed double orientation,

a Zeiss universal stage was used to measure birefringence as a function of tilt angle,  $\phi$ , by rotation about the draw axis<sup>16,17</sup>. The sample was placed in between glass hemisphere of 1.555 refractive index for beam convergence. This limits  $\phi$  measured up to 40°.

A flat film Statton camera with a sample-to-film distance of 5 cm and 32 cm was used to obtain wide- and small-angle x-ray diffraction (WAXD and SAXS) photographs respectively using Cu K $\alpha$  radiation with Ni filter, operating at 40 kV and 30 mA. Intensity of x-ray film was measured with a Nonius microdensitometer.

Crystallite size in a-axis direction was measured from broadening of (200) diffraction with a Siemen D-500 diffractometer equipped with a scintillation counter. The divergence and anti-scatterer slits were 0.3° and the receiving slit was 0.015°, with scanning at 0.2° 2 $\theta$ /min. The hexamethylene tetramine peak at 17.8° 2 $\theta$  was used to correct for instrumental broadening. Scherrer equation was used to calculate the crystallite size.

## RESULTS AND DISCUSSION

Characterization of Undrawn Gel Film. Nylon 6 was found to gel into the  $\alpha$ -crystals with a high crystallinity, 55%, as measured from DSC. This crystal form is the one normally obtained by solution crystallization. A DSC scan of a thoroughly dried gel (Figure 1) shows two prominent endotherms with peak melting point at 210 and 219.5°C. The two endotherms have approximately equal peak area. Double endotherms in solution crystallized Nylon 6 have previously been reported<sup>18,19</sup>. Kyotani<sup>19</sup> attributed the low temperature endotherm to lamellar crystals which crystallized during cooling the solution to room temperature after isothermal crystallization. Prolonging the isothermal crystallization time was reported to give only a single high temperature endotherm of more perfect, larger lamellar crystals. However, Stamhuis and Pennings<sup>13</sup> had shown that Nylon 6 gel morphology exhibits long ribbons of aggregated fibrillar crystals. This fibrillar morphology was also obtained from stirred crystallization in 1,2,6-hexanetriol solution giving a melting point of 223 ~ 224°C<sup>19</sup>. Thus in the present gel system, the observed high temperature endotherm is likely for fibrillar crystals mixed with possibly some large lamellar crystals.

Figure 2 shows WAXD and SAXS photographs of a dried gel film prior to extrusion draw. The x-ray beam was directed perpendicular and parallel to the film plane. Viewed perpendicularly, Figure 2(a), there are two (200) and (002) isotropic rings. The inner (200) reflection is much more intense than the outer (002) reflection. SAXS however shows that over a larger range, the system is not entirely isotropic as indicated by an uneven intensity for the ring. When

the x-ray beam is placed parallel to the film plane, Figure 2(b), wide equatorial (200) and (002) arcs are superimposed on the Debye rings, and SAXS shows wide meridional maxima. These indicate that orientation has been introduced in the gel film with the b-chain axis weakly oriented perpendicular to the film plane as a result of squeezing during solvent removal. This is confirmed by WAXD photograph, taken with the beam parallel to an unpressed gel, which shows only isotropic rings. The preorientation, however, does not cause double orientation of crystals in the drawn gel, to be discussed later. It does affect the distribution of crystals when viewed parallel to the draw direction.

#### Properties of Drawn Gel Film

Thermal evaluation by DSC of the drawn gel film is shown in Figure 1. With increasing draw ratio, the low temperature endotherm decreases in magnitude and shifts slightly towards higher temperature, completely disappearing at a draw 4.6X and onwards, leaving only a single endotherm with a peak melting at 224°C at draw 5.4X. The disappearance of the low temperature endotherm must be due to the destruction of these lamellar crystals on draw leading to their incorporation in a newly-formed fibrous morphology. The fate of the ribbons of fibrillar crystals on draw is not revealed by DSC since its melting point is in the same range as that of the drawn fibrous morphology<sup>20</sup>. The fraction of crystallinity decreases with draw by ~9% at the highest draw ratio 5.7 (Table 1). A major decrease has also been reported for crystalline poly(ethylene terephthalate)<sup>21</sup> with yet no satisfactory explanation.

As pointed out earlier, Nylon 6 gel formation does not necessarily result in significant reduced molecular entanglement. The maximum draw ratio of 5.7 obtained here is comparable to those previously reported for Nylon 6. Tensile moduli of the drawn gel are shown in Figure 3. The moduli of solvent cast film, drawn under similar conditions, shown by the broken line, are included for comparison. At equivalent draw ratios, the modulus of gel film is modestly higher, reaching 5.6 GPa. Annealing at 190°C under tension shows a slight improvement in the modulus, from 5.0 GPa to 5.7 GPa for draw ratio 3.7.

The total orientation of both the amorphous and crystalline chains was measured by birefringence (Figure 4). The undrawn film shows birefringence of 0.011, which is due to orientation introduced during solvent removal. On drawing, the birefringence increases, almost linearly to 0.044 at a draw of 5.7. However, the drawn cast film shows a marked increase in birefringence at low draw, reaching a plateau of 0.061 at a draw of 3.5 with values consistent with reports on uniaxially drawn Nylon 6 film and filament<sup>22</sup>. The lower birefringence of the drawn gel is consistent with investigations by both WAXD and SAXS which show double orientation; there are two populations of crystals with chain axis either parallel or perpendicular to the draw direction. Since birefringence is the difference in refractive indices along and perpendicular to draw, the presence of crystals with chain axis perpendicular with draw direction reduces the birefringence.

#### Deformation Mechanism

Double orientation on deformation has been reported for several types of gel<sup>23,24,25</sup>. An elegant explanation has been offered by Keller<sup>12</sup> in which the

initial gel contains a mixture of both micellar and lamellar crystals. On deformation, the micellar crystals orient with their chain axis in the draw direction as in the stretching of a network. Conversely, the lamellar crystals align with their lamellar planes along the stretch direction and therefore with chain axis perpendicular to draw. An unconnected lamellar crystal could possibly orient this way on drawing without much chain unravelling. It is less likely that lamellar crystals, presumably with interconnections, will do so rather than orienting with chain unravelling to form fibrous morphology in the draw direction.

Since gelation of Nylon 6 is caused by the interlacement of fibrillar crystals, we propose an alternative mechanism for draw of Nylon 6 gel. Orientation of crystals with chain axes in the draw direction arises from the fibrous morphology normally observed in uniaxial drawing. The second orientation of crystals, with chain axis perpendicular to draw direction, are from the fibrillar crystals which have chain axis perpendicular to surface plane and hydrogen bonding in the long axis. They rotate when subjected to torque on deformation so that the long axis (a-axis) is preferentially oriented in the draw direction. This is similar to the rotation of needle shape crystals in segmented polyurethane to give a negative orientation as proposed by Bonart<sup>26</sup>. We have shown that this proposed mechanism is consistent with both the WAXD and SAXS study as a function of draw ratio for the gel.

Figure 5 shows a series of WAXD photographs of gel film with increasing draw ratio: the x-ray beam is normal to film plane. The undrawn film shows

FIGURE CAPTIONS




- FIGURE 1: Thermal Behavior by DSC of Undrawn and Drawn Nylon 6 Gel Film
- FIGURE 2: WAXD and SAXS Photographs of Undrawn, Dried Gel with Beam,  
(a) Normal and (b) Parallel to Film Plane
- FIGURE 3: Tensile Modulus as a Function of Draw Ratio  
 Solvent-Cast Nylon 6 Film,  
 Nylon 6 Gel Film,  
● Gel Film After Annealing
- FIGURE 4: Birefringence as a Function of Draw Ratio  
 Nylon 6 Gel Film,  
● Solvent-Cast Nylon 6 Film
- FIGURE 5: WAXD Photographs of Gel Film with Increasing Draw Ratio.  
X-ray Beam Normal to Film Plane
- FIGURE 6(a) & (b): Reciprocal Lattice Representation of Nylon 6  $\alpha$ -Crystal Showing Relative Position of (200), (002) and (202) Reflections in WAXD. (a) Low draw,  $<1.9x$ , (b) high draw,  $>3.7x$ .
- FIGURE 7: SAXS Photographs of Gel Film with Increasing Draw Ratio.  
X-ray Beam Normal to Film Plane

TABLE 4

Change of Angle,  $\Psi$ , Between Long Axis of  
Fibrillar Crystals and Draw Direction

<u>Draw Ratio</u>	<u><math>\Psi^\circ</math></u>
1.3	23.6
1.9	12.0
2.1	10.1
2.8	9.2
3.7	0



TABLE 3  
Long Period, I, From SAXS of Gel Film With  
Increasing Draw Ratio

	<u>L (A)</u>		
<u>Draw Ratio</u>	<u>Equatorial</u>		<u>Meridional</u>
Undrawn	64		
1.3	66	66	87
1.9	66	65	86
2.1	68	66	87
2.8	66	66	85
3.7	65		87
4.6	62		82
5.4	62		81

TABLE 2

Crystallite Sizes Along a-axis and Intensity Ratio,  
 $I_{200}/I_{002}$ , of (200) and (002) Equatorial Reflections  
with Increasing Draw Ratio

Draw Ratio	Crystallite Size $\bar{D}_{200}$ (Å)		$I_{200}/I_{002}$
	Equatorial	Meridional	
Undrawn	104		0.69
1.9	64	101	0.70
3.7	62	91	0.81
4.6	69	82	1.00
5.4	69	91	1.20

TABLE 1

Change of Crystallinity as a Function of  
Draw Ratio as Measured by DSC

<u>Draw Ratio</u>	<u>% Crystallinity</u>
Undrawn	55.0
2.1	47.8
2.9	48.7
3.7	47.3
4.6	45.6
5.4	45.0
5.7	45.5

15. A.E. Zachariades, P.D. Griswold and R.S. Porter, Polym. Eng. Sci., 19, 441 (1979).
16. R.S. Stein, J. Polym. Sci., 24, 383 (1957).
17. C.R. Desper, Ph.D. Thesis, University of Massachusetts, 1966.
18. T. Shimada and R.S. Porter, Polymer, 22, 1124 (1981).
19. M. Kyotani, J. Macromol. Sci., Phys., B21, 275 (1982).
20. M. Todoki and T. Kawaguchi, J. Polym. Sci., Phys. Ed., 15, 1507 (1977).
21. J.R.C. Pereira and R.S. Porter, J. Polym. Sci., Phys. Ed., 21, 1147 (1983).
22. F. Fujimoto et.al., Nippon Sen'i Kikai Gakkai, 19, 1 (1973).
23. H. Berghman, F. Govaerts and N. Overbergh, J. Polym. Sci., Phys. Ed., 17, 1251 (1979).
24. S.J. Guerrero, A. Keller, P.L. Soni and P.H. Geil, J. Polym. Sci., Phys. Ed., 18, 1533 (1980).
25. E.D.T. Atkins et.al., Colloid Polym. Sci., 262, 22 (1984).
26. R. Bonart and K. Hoffmann, Colloid & Polym. Sci., 260, 268 (1982).
27. B. Wunderlich, "Macromolecular Physics, Vol. I", Academic Press, 1973.

REFERENCES

1. A.J. Pennings and K.E. Meihuizen, in "Ultra-High Modulus Polymers", A. Ciferri and I.M. Ward, Editors, Applied Science, 1979.
2. P.J. Barham, *Polymer*, 23, 1112 (1982).
3. M.R. Mackley and G.S. Sapsford, in "Developments in Oriented Polymers-I", I.M. Ward, Editor, Editor, Applied Science, 1982.
4. P. Smith and P.J. Lemstra, *J. Polym. Sci., Polym. Phys. Ed.*, 19, 1007 (1981).
5. M. Matsuo and R. St. John Manley, *Macromolecules*, 15, 985 (1982).
6. C.G. Cannon, *Polymer*, 23, 1123 (1982).
7. A. Peguy and R. St. John Manley, *Polymer Commun.*, 25, 39 (1984).
8. D.T. Grubbs, 4th Cleveland Macromolecule Symposium, June, 1983.
9. D.J. Lloyd, in "Colloid Chemistry, Vol. I", J. Alexander, Editor, New York, 1926 (quoted in Ref. 11).
10. A. Tager, "Physical Chemistry of Polymers", MIR Publications, 1978.
11. P.H. Hermans, in "Colloid Science, Vol. II", H.R. Kuryt, Editor, Elsevier, 1949.
12. A. Keller, in "Structure-Property Relationships of Polymeric Solids", A. Hiltner, Editor, Plenum Press, 1983.
13. J.E. Stamhuis and A.J. Pennings, *British Polym. J.*, 10, 221 (1978).
14. H.H. Chuah and R.S. Porter, *J. Polym. Sci., Phys. Ed.*, 22, 1353 (1984);  
A.E. Zachariades, M.P.C. Watts, T. Kanamoto and R.S. Porter, *J. Polym. Sci., Polym. Lett. Ed.*, 17, 485 (1979).

annealing, because of reorientation, the annealed samples not only have higher birefringence but also increase with tilt angle. The increase is linear for draw 2.9X up to the angles measured but show tendency of reaching plateau in draw 3.7X. For a biaxial orientation, birefringence at  $\phi = 0^\circ$  is different from at  $\phi = 90^\circ$ . Plot of birefringence vs.  $\sin^2\phi$  is linear and extrapolation to  $\sin^2\phi = 1$  gives birefringence of the other axes pair<sup>17</sup>. Although annealed 2.1X film shows a linear increase, it is uncertain that this can be extrapolated to imply biaxial orientation, especially the annealed 3.7X film shows non-linear increase. Therefore, reorientation on annealing produced a much more complicated overall orientation.

#### CONCLUSIONS

Partially dried Nylon 6 gel film was drawn by co-extrusion with poly(oxyethylene) as outer billet at 150°C in an Instron rheometer up to a maximum draw ratio of 5.7X. Tensile moduli are comparable to those obtained in a drawn solvent-cast Nylon 6. The drawn gel film showed a double orientation with one population of crystals oriented with chain axis in the draw direction. These crystals originated from the drawn fibrous morphology. The other crystal population had chain axis perpendicular to draw direction and identified as the fibrillar crystals that cause gelation. A deformation mechanism leading to this double orientation, is proposed from the study of birefringence, WAXD and SAXS. Annealing at 190°C causes reorientation of the fibrillar crystals resulting in a more complex orientation.

#### ACKNOWLEDGEMENT

We wish to express appreciation to the Office of Naval Research for the support of this research.

not the molecular chain. At low draw, Figure 8(b) shows the long axes partially oriented towards the draw direction. Since the fibrillar crystals are distributed about the draw direction, this arrangement gives four-point SAXS pattern at the equator. On further drawing, Figure 8(c), the long axes are in the draw direction; the four-point scattering merges into two equatorial scatterings. Superimposed on this, the simultaneous development of fibrous morphology gives the meridional scatterings, therefore, a resultant four-point scattering of Figure 7.

#### Annealing Behavior

The drawn gel films were annealed under tension at 190°C for 3 hours. The modulus and birefringence increase slightly (Figures 3 and 4). WAXD and SAXS with x-ray beam in normal and transverse directions are not significantly different from that of unannealed samples. However, when the beam is in the draw direction, superimposed on both (200) and (002) rings are intense arcs at the equator similar to that of undrawn state of Figure 2. Reorientation of the fibrillar crystals occurs on annealing with chain axis partially reoriented normal to film plane. Crystals that randomize around the draw direction must be in a metastable state. Annealing reverses the process, resulting in a more complicated orientation.

Birefringence of both unannealed and annealed gel film of draw 2.1X and 3.7X are shown in Figures 9(a) and (b) as a function of tilt angle,  $\phi$ . For unannealed samples, there is only a slight increase in birefringence with  $\phi$  indicating a slight departure from isotropy around the uniaxial draw axis. On

equatorial periodicity of the fibrillar crystals is smaller however but remains fairly constant at ~65 Å on draw. Although Stamhuis and Pennings<sup>13</sup> reported the lateral dimension of such crystals to be 100~200 Å, thickness in the chain direction was not reported. The present periodicity is within the range for lamellar thickness reported for solution grown Nylon 6 crystals<sup>27</sup>.

The split angle,  $\Psi$ , of the equatorial scattering maxima gives the average angle of the long axis of fibrillar crystals to the draw direction. At a draw of 1.3X, the angle is 23.6° and decreases to 0° at 3.7X (Table 4). At 0° angle, the long axis (a-axis) of the fibrillar crystals is completely oriented in the draw direction. The SAXS results support the observation from WAXD.

From both WAXD and SAXS study, we showed double orientation in the drawn gel film. One population of crystals has chain axis parallel to the uniaxial draw direction. This type of crystals belong to the fibrous morphology normally found in tensile drawing. The other crystal population has a chain axis perpendicular to draw, and they are identified as the fibrillar crystals associated with gelation. They rotate when subjected to torques during deformation, with the long axis orienting towards the draw direction. Because hydrogen bond is also in the long axis, chains resist drawing until later stages when "fracture" possibly occurs and transform partly into fibrous morphology. This causes the depletion of the fibrillar crystals and therefore decrease in intensity in both their WAXD and SAXS. Figure 8 is a schematic of ribbons of these fibrillar crystals undergoing deformation with long axis rotating towards the draw direction. The lines represent fibrillar crystals, bundle into large ribbon, and



(202) reflections. The crystallite sizes of fibrillar crystals along a-axis, as measured from broadening of meridional (200) reflection, showed a slight decrease on draw, from 101 Å at 1.9X to 82~91 Å at higher draw. For equatorial (200) reflection, the crystallite sizes remain fairly constant on draw, 62~69 Å. This dimension may be interpreted as the lateral size of the drawn microfibril. Consider the interchain dimension of 4~5 Å, arithmetically, this corresponds to about 15 Nylon 6 chains in close lateral packing. This number indicates that the equatorial (200) reflection is unlikely the result of drawn micellar crystals network.

While the WAXD study gives us information of how chains are oriented at the level of unit cell axes, SAXS provides a view on orientation at the larger lamellar level. Figure 7 shows SAXS patterns of gel film with increasing draw ratio. At a low draw of 1.3X, there is a marked change of the scattering pattern from nearly isotropic scattering for the undrawn state to a discrete four-point pattern along the equator. At higher draw, the four-point moves closer, while meridional scattering develops at 1.9X, thus giving a six-point scattering pattern. On further draw, the equatorial four-point merges into two-points at 3.7X, giving a final four-point scattering along the meridian and equator.

To show that the equatorial scattering is not due to voids, the drawn film was immersed in benzyl alcohol (refractive index 1.54) for 14 days. It was then coated with paraffin oil to reduce solvent evaporation under vacuum while taking SAXS patterns. The patterns found are the same, indicating the equatorial scattering is not due to voids.

The measured lamellae long periods are tabulated in Table 3. The meridional long period of the drawn fibrous morphology is constant at ~85 Å. The

by a reciprocal lattice as in Figure 6(b). In this case the meridional (200) reflections show intensity maxima at an angle of  $22.5^\circ$  from the draw direction, which is indeed observed from draw ratio 3.7X onwards indicating a complete a-axis orientation of the fibrillar crystals in draw direction. A weak (202) reflection appears diagonally in the reciprocal lattice and is also observed in the diffraction pattern.

If we now superimpose in Figure 6(b) the equatorial (200) and (002) reflections from the normal fibrous morphology with chain axis in draw direction, the composite pattern is consistent with observations for a draw 3.7X of Figure 5. Only the (002) reflection appears from crystals with both orientations, and therefore its intensity must be enhanced. For isotropic  $\alpha$ -crystals, the intensities of (200) and (002) reflections are nearly equal. Table 2 shows that the ratio of intensities,  $I_{200}/I_{002}$ , for (200) and (002) equatorial reflections is 0.69 and increases to 1.20 at a draw 5.4X. The increase in this intensity ratio is a result of randomization of fibrillar crystals around the draw axis and at high draw ratio, the eventual fracture of these crystals to orient in the draw direction.

Crystallite sizes along a-axis for both types of crystal orientations, are measured from WAXD (200) line broadening, and are shown in Table 2. Scherrer's equation was used after correction for instrumental broadening. It is assumed that broadening is due to crystallite size alone, neglecting lattice distortion. Therefore, the measured sizes are a lower limit. Measurement of (002) broadening is not suitable, as it is not a pure peak containing a mixture of

draw direction. The meridional (200) reflections are, however, from crystals with chain axis oriented perpendicular to draw. These reflections are suggested here, to be from the fibrillar crystals which have chain axis perpendicular to their flat surfaces.

To show how these diffraction patterns are obtained for these crystals, we have constructed a reciprocal  $a^*-c^*$  lattice for the fibrillar crystals with chain axis oriented perpendicular to the draw direction. Since WAXD patterns are taken with a flat film camera and with Cu  $K\alpha$  radiation of wavelength 1.54 Å, the surface of the Ewald sphere curved. The flat film diffraction pattern is then a distortion of the reciprocal lattice representation. Nevertheless, it is useful to show the relative location of the reflections arising from orientation.

The reciprocal lattice is oriented such that the (002) reflection is at the equator, while the (200) reflection is at the meridian (Figure 6a). At low draw, the fibrillar crystals rotate when subject to torques. The  $a$ -axis orients towards the draw direction. Since  $c^*$ -axis is perpendicular to the  $a$ -axis, the measurement of the angle  $\Psi$  of (002) reflection from the equator indicates the angle at which the  $a$ -axis is tilted towards the draw direction. Because of wide angular spread of the  $a$ -axis, we expect a spread of  $\Psi$  with (200) and (002) reflections smeared over the meridian and equator, respectively. This results in WAXD patterns for draw  $<1.7\times$  as shown in Figure 5.

At higher draw, when the  $a$ -axis of the fibrillar crystals are oriented in the draw direction,  $\Psi$  becomes  $0^\circ$ . The diffraction pattern is then represented

isotropy with (200) and (002) Debye rings. The outer (002) reflection is mixed with (202), for convenience, we refer to this as (002) only. At low draw ratio, up to 1.7, the inner (200) reflection forms meridional arcs with broad azimuthal spread, while the outer equatorial (002) arcs are also broad but less intense. At a draw ratio of 1.9, the spread of these two arcs becomes narrower with simultaneous development of a faint (200) reflection at the equator. These equatorial arcs become prominent at a draw 2.9X while the meridional (200) arcs become narrower in spread and split with maximum intensity centered at  $\sim 22^\circ$  angle to the extrusion direction. Correspondingly, the azimuthal spread of (002) also becomes narrower. There is a faint reflection located diagonally with spacing nearly the same as that of the outer (002) reflection, which we identify as a weak (202) reflection. At higher draw of 4.6, the intensity of meridional (200) arcs decreases sharply when compared to its equatorial reflection.

Because of the complex orientation, we also examined both WAXD and SAXS with the x-ray beam transverse and parallel to the draw direction. The transverse diffraction shows similar patterns as that of normal beam. At low draw, the parallel direction diffraction shows a weak orientation introduced during squeezing in gel film preparation with broad equatorial (200) arcs. On further drawing to 3.7X, it develops into a ring of uneven intensity showing tendency of randomization around the draw direction; so the system can be described as having double orientation of the crystals but to some extent, isotropic around the draw direction at higher draw.

In Figure 5, the equatorial (200) and (002) reflections can be identified as from the normal fibrous morphology with chain axes parallel to the uniaxial

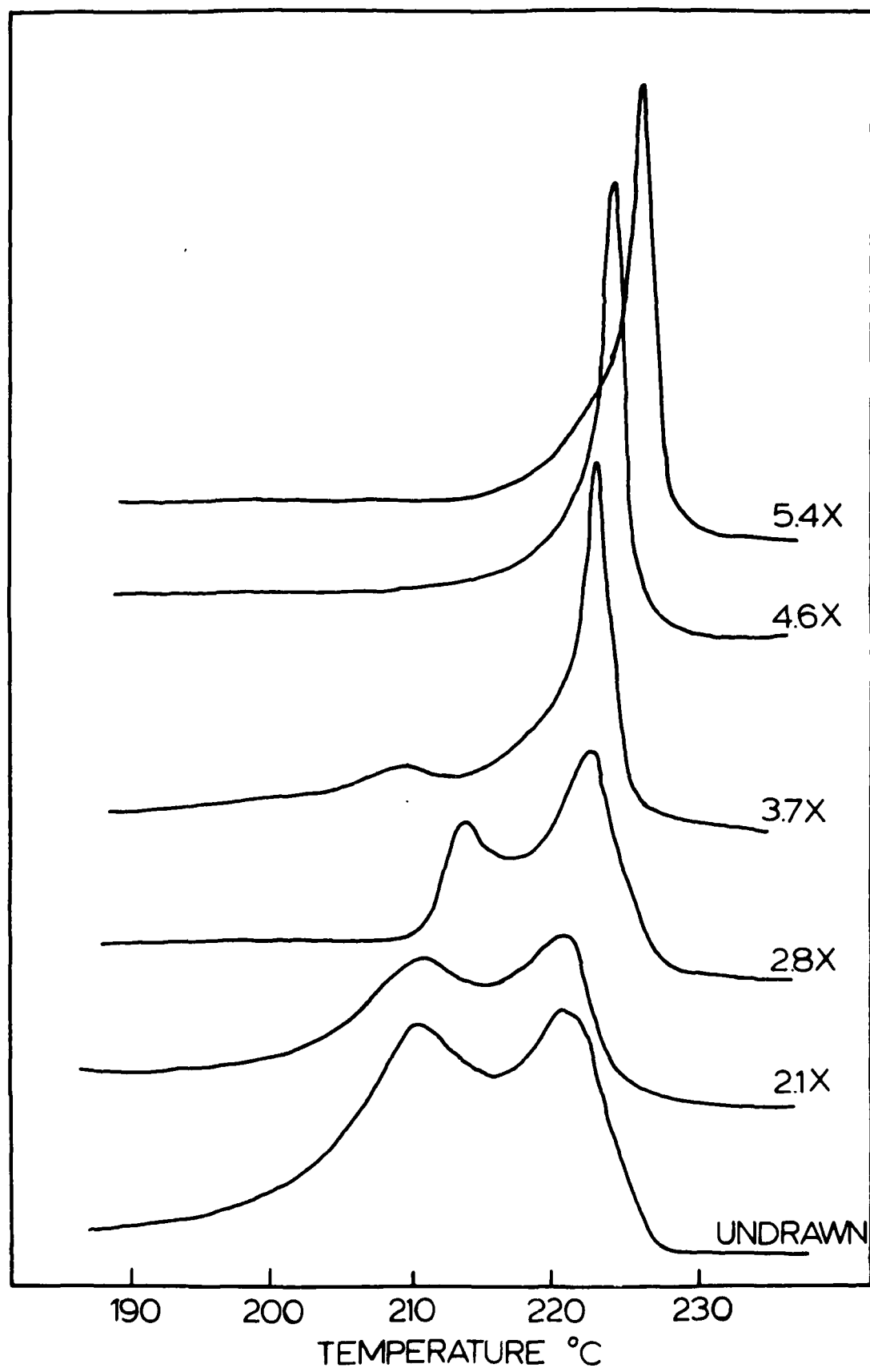
FIGURE 8: Schematic Representation of Orientation of Fibrillar Crystals During Deformation

- (a) Undrawn State with Random Interlacement of Fibrillar Crystals
- (b) Low Draw Ratio  $\leq 1.9X$ , Long Axis (a-axis) of Fibrillar Crystals Orienting Towards Draw Direction
- (c) High Draw Ratio, long axis of Fibrillar Crystals in Draw Direction
- (d) Enlargement of Aggregate of Fibrillar Crystals Showing the Long Period

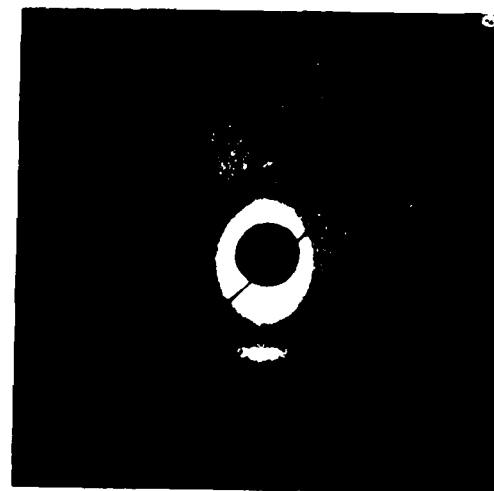
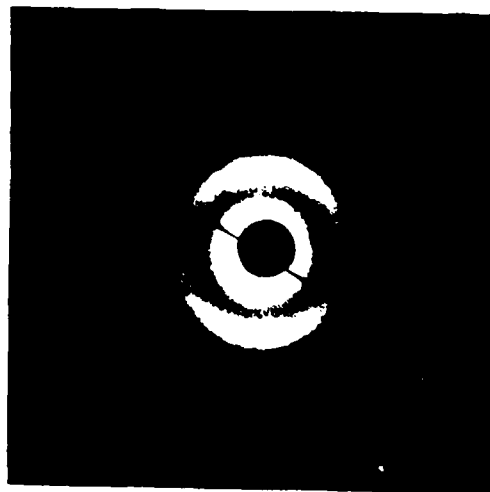
FIGURE 9: Birefringence as a Function of Tilt Angle  $d$  for Unannealed (■), and Annealed (●) Drawn Gel

- (a) Draw Ratio 2.9
- (b) Draw Ratio 3.7

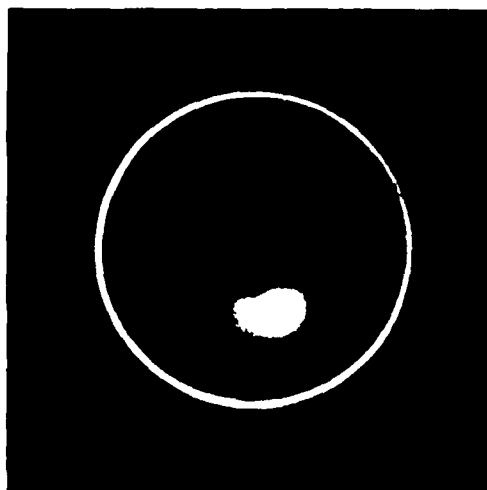
ENDOTHERM  $\longrightarrow$



SAXS

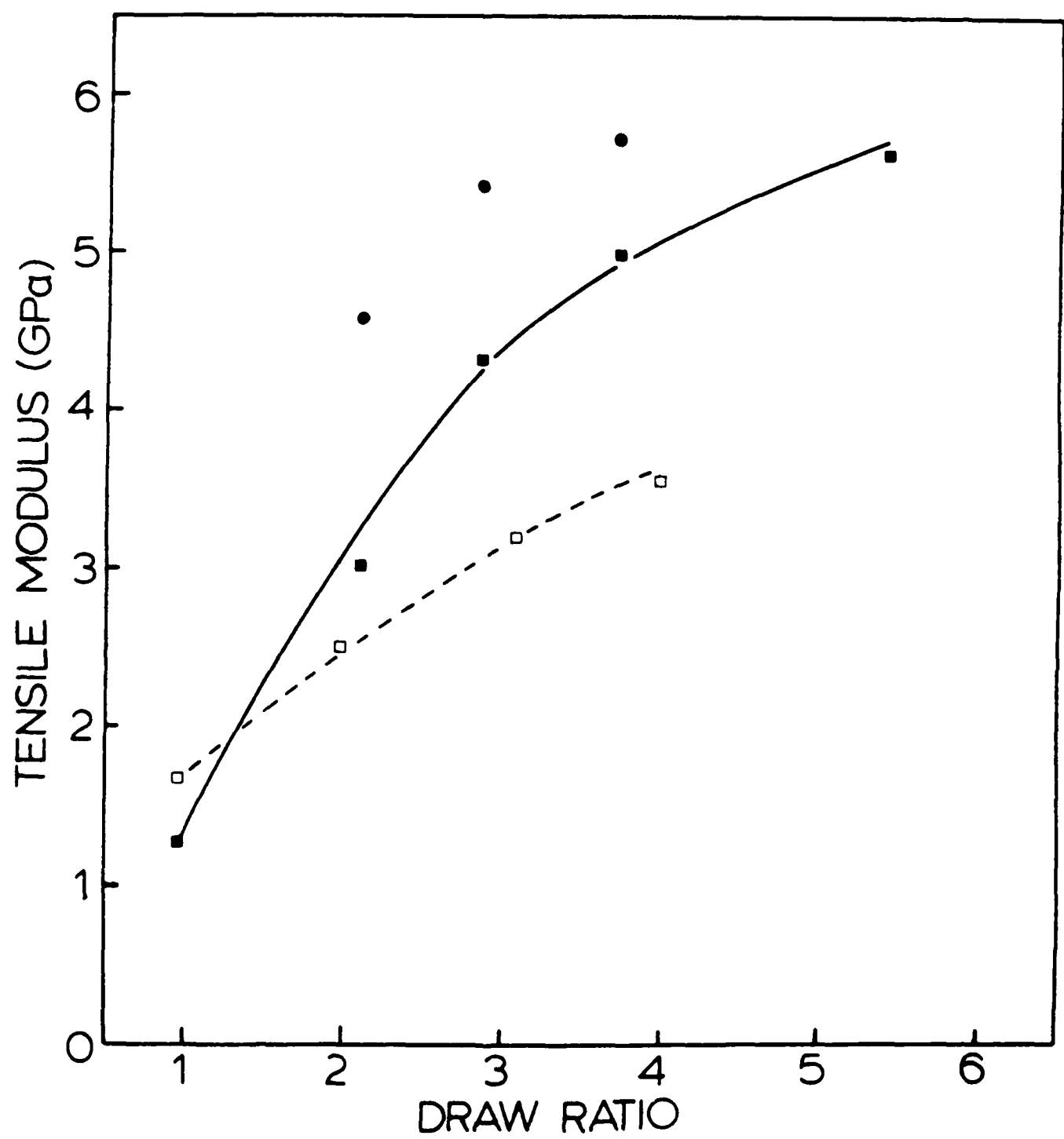


WAXD

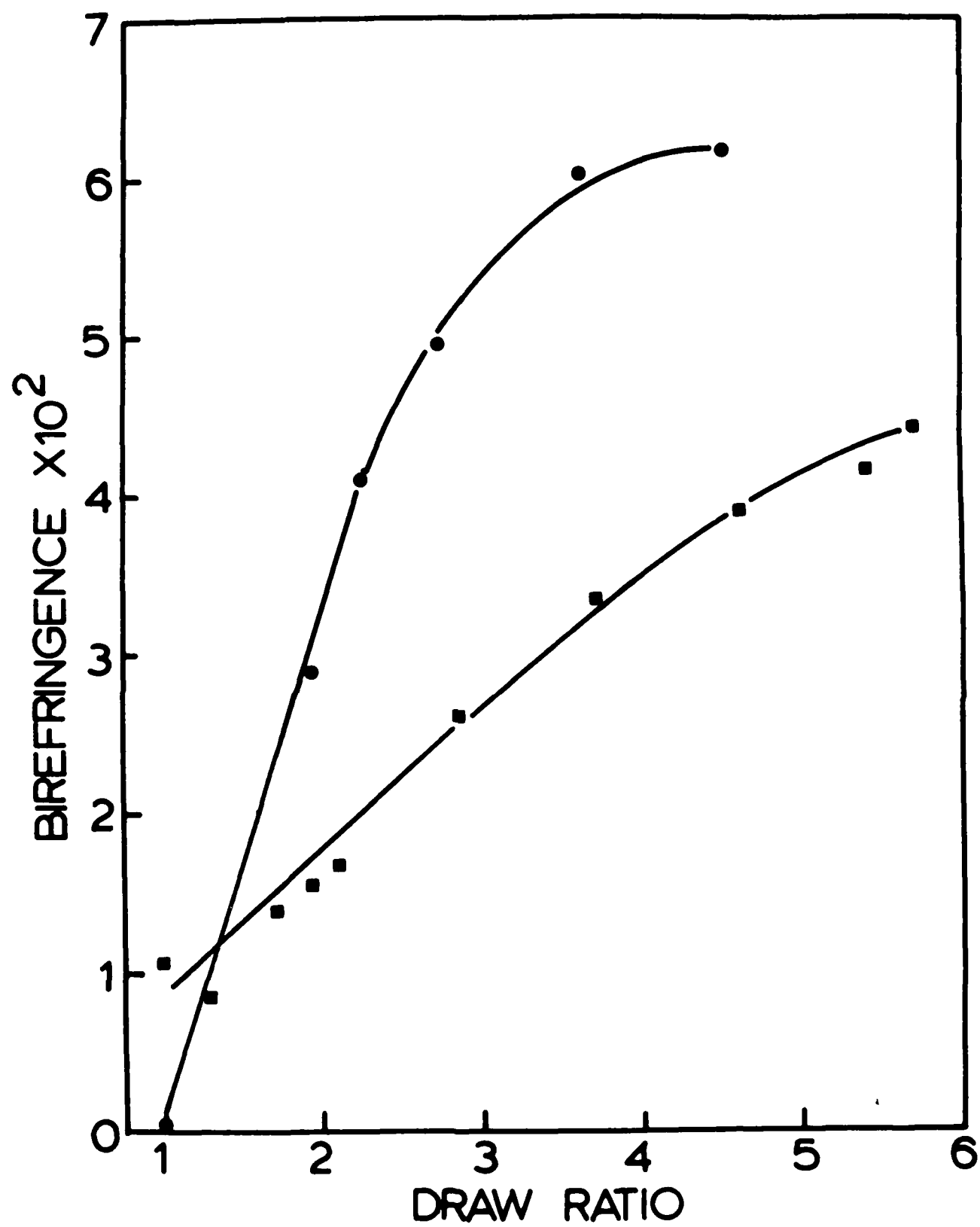


(a)

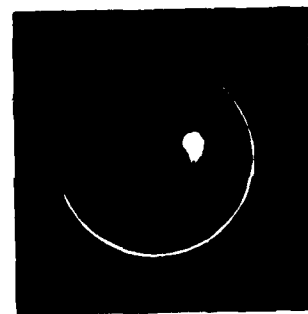
(b)



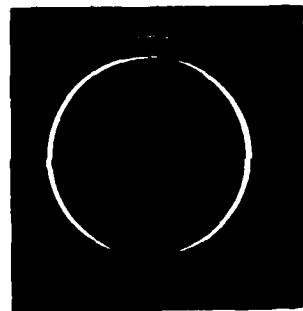




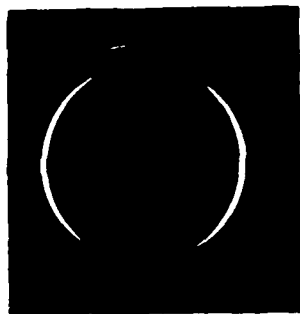
EXTRUSION DIRECTION



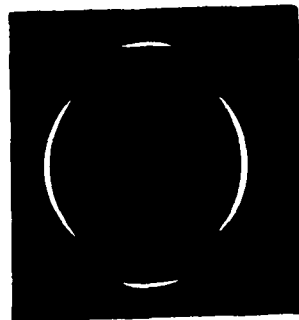
UNDRAWN



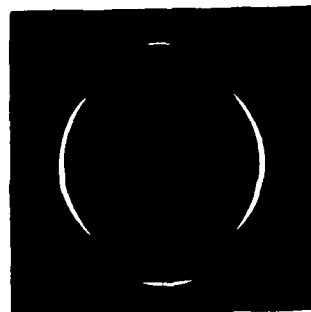
1.3X



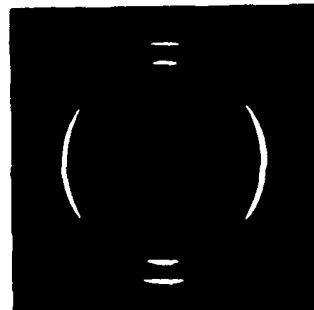
1.7X



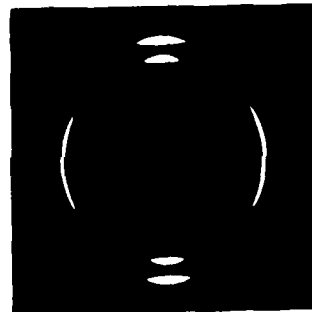
1.9X



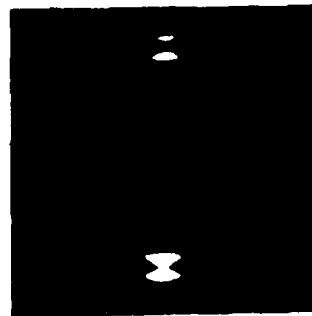
2.1X



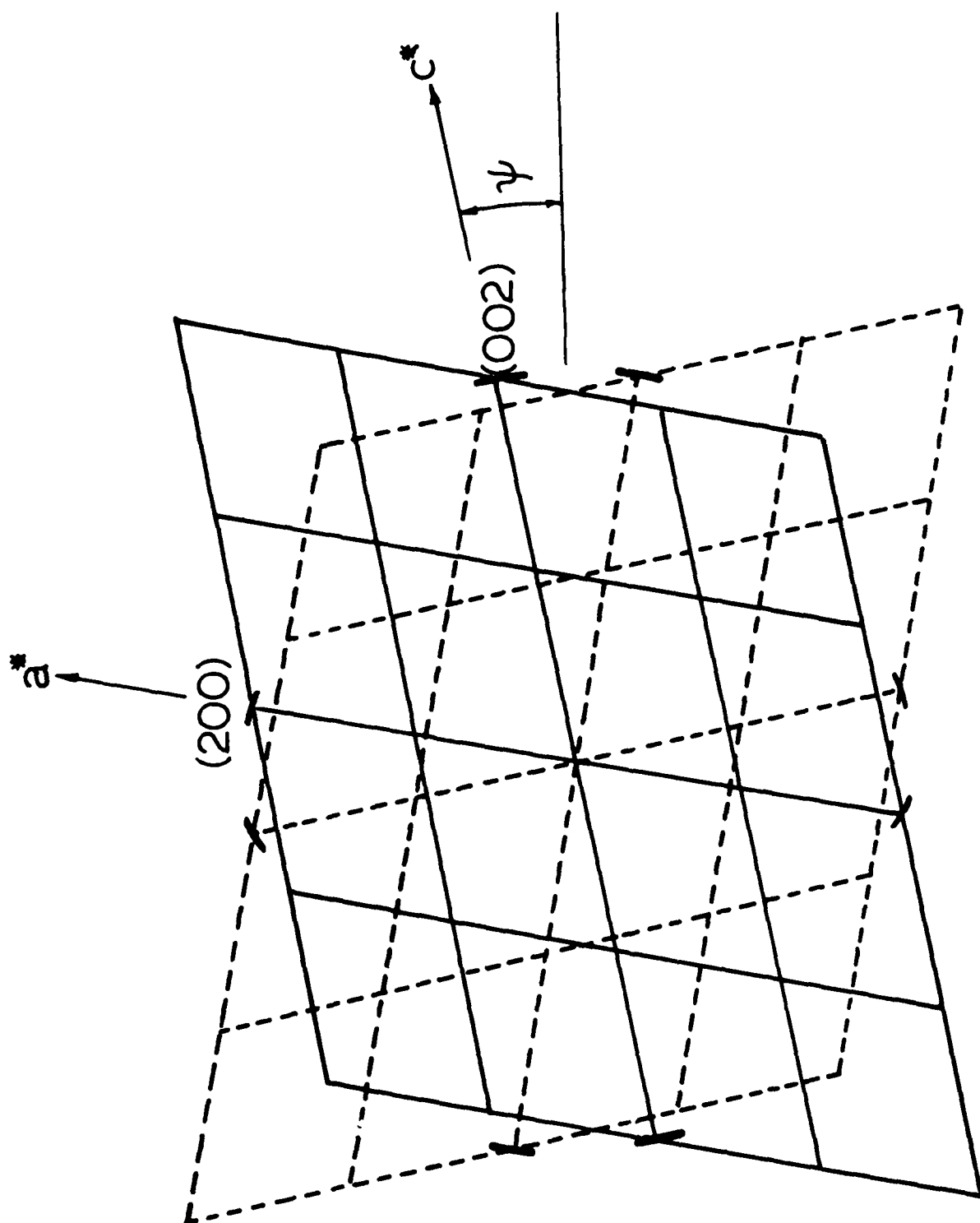
2.9X

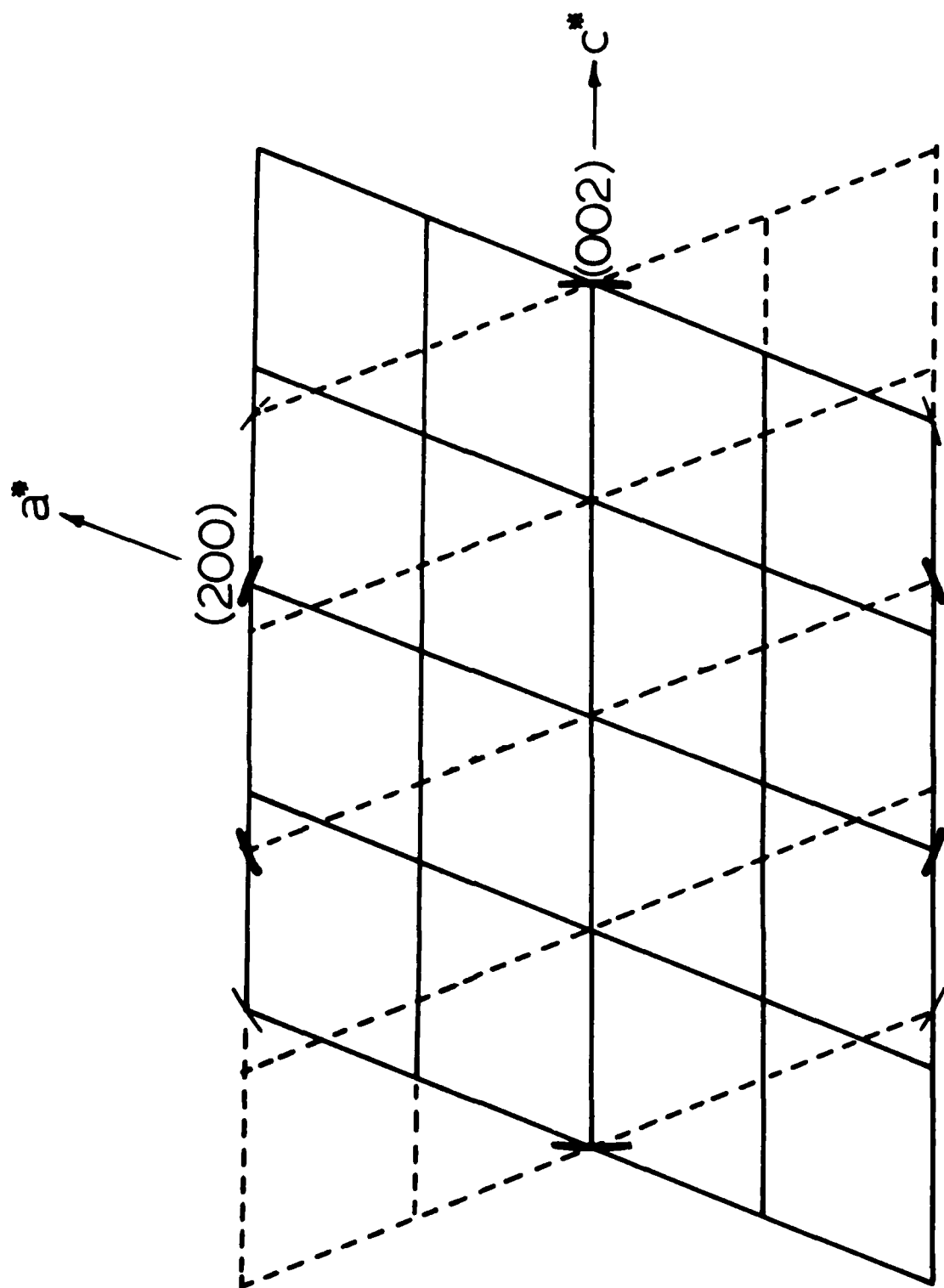


3.7X

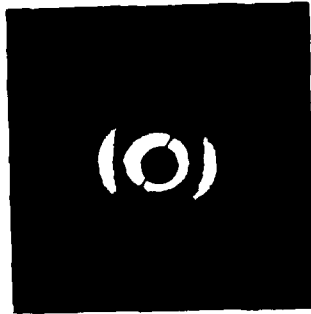


4.6X

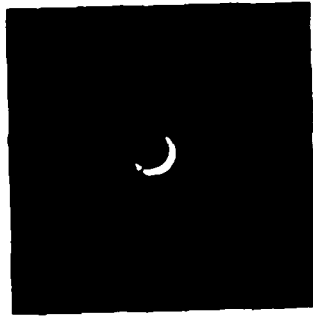




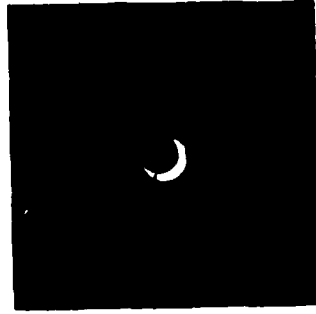
EXTRUSION DIRECTION  
←



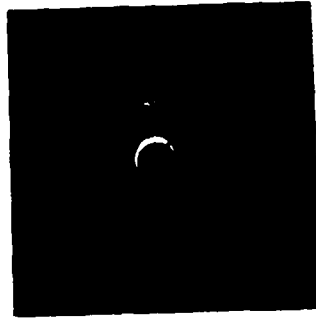
UNDRAWN



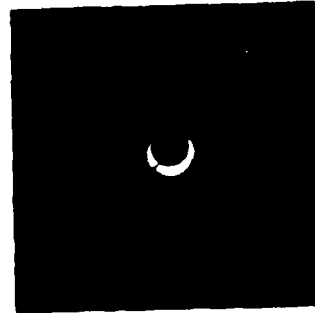
1.3X



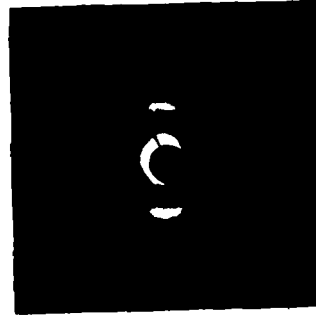
1.7X



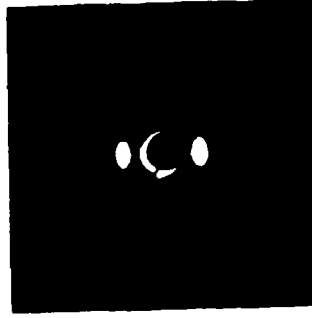
1.9X



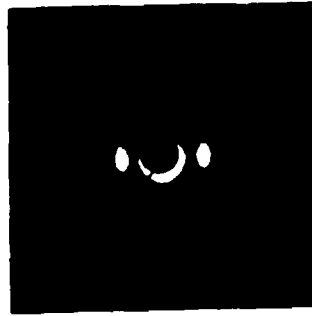
2.1X



2.9X

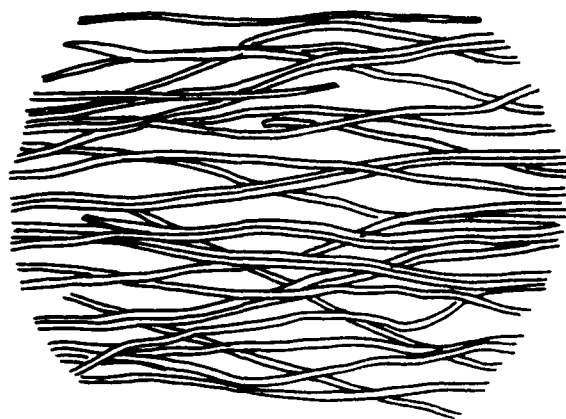


3.7X

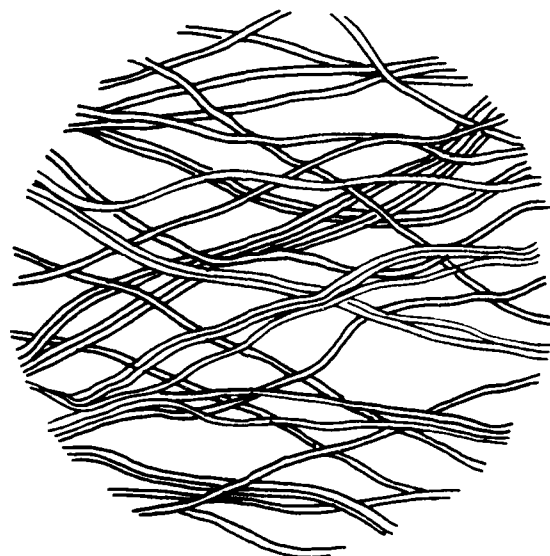


4.6X

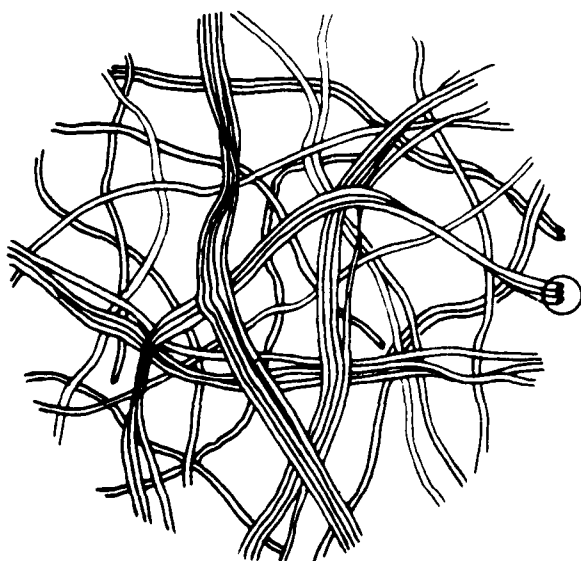
(c)



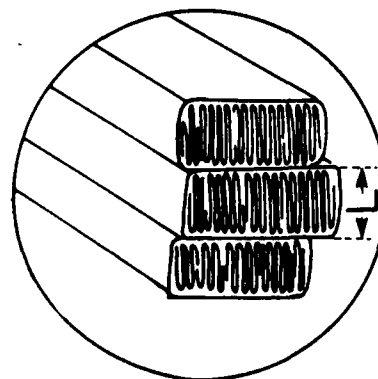
(b)



(a)

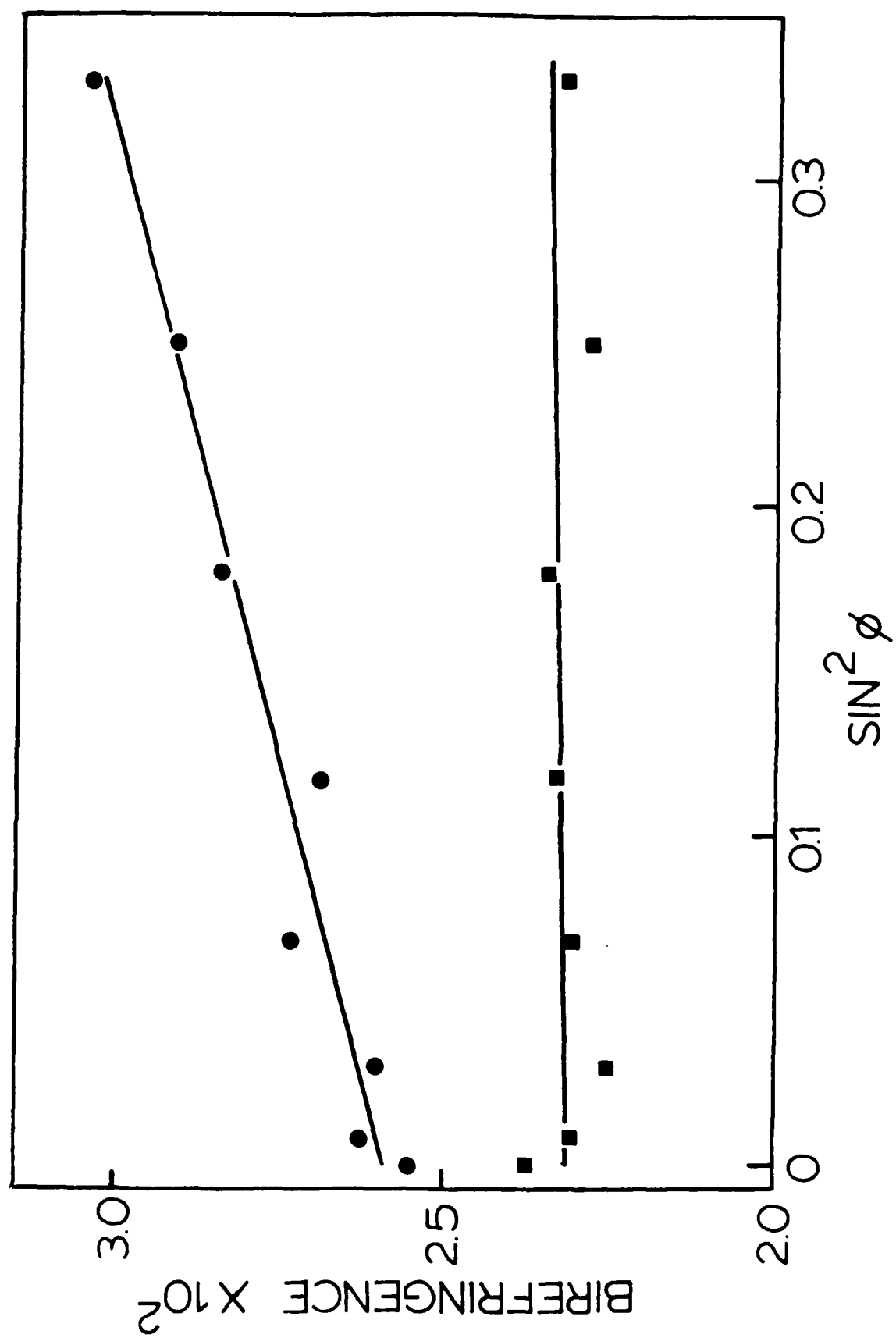


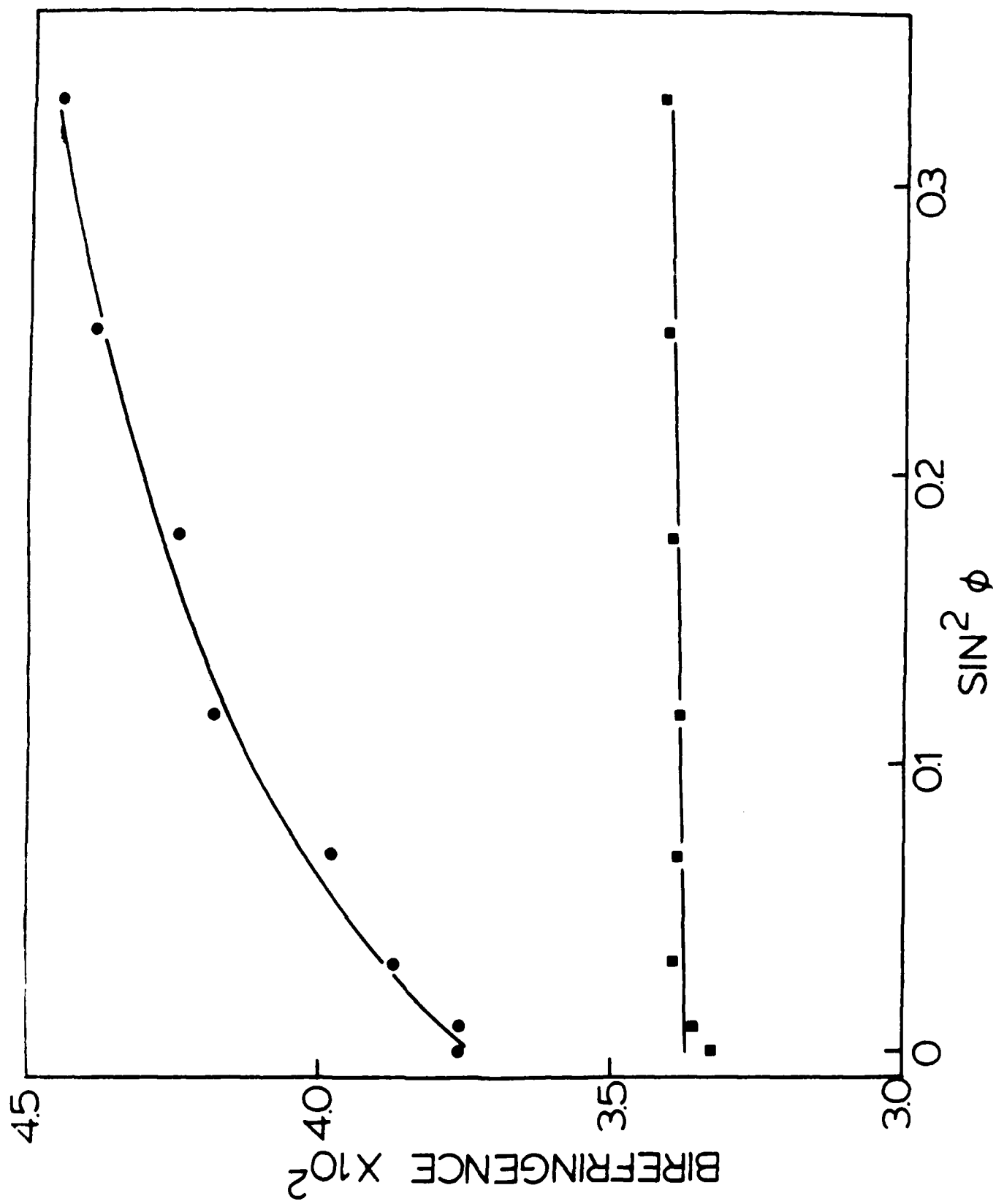
(d)



Extrusion Direction









**END**

**FILMED**

**8-85**

**DTIC**